

and impurity radiation effects than fuel added more deeply as with pellet injection. It also demonstrates that pellet fueling is more efficient than gas puffing.

We have demonstrated that relatively large pellets can be injected into a tokamak plasma, resulting in substantial increases in density. The advantages which may arise from this technique are twofold: (1) The technological difficulties associated with fueling by injection of pellets at high velocity may be eased because for a given penetration depth, large pellets require lower velocities than do smaller pellets, and (2) fueling by deep pellet injection appears to be more efficient from the point of view of plasma heating requirements than does edge fueling by gas injection.

The authors wish to acknowledge the assistance of the Tokamak Experimental Section and in particular C. E. Bush, J. L. Dunlap, R. C. Isler, P. W. King, D. H. McNeill, J. T. Mihalczko, and J. B. Wilgen. The discussions with and contribu-

tions of H. C. Howe and M. Murakami are also gratefully acknowledged. This research was sponsored by the Office of Fusion Energy (ETM), U. S. Department of Energy under Contract No. W-7405-eng-26 with the Union Carbide Corporation.

<sup>1</sup>C. A. Foster, R. J. Colchin, S. L. Milora, K. Kim, and R. J. Turnbull, *Nucl. Fusion* **17**, 1967 (1977).

<sup>2</sup>W. Amenda, K. Büchl, R. Lang, L. L. Lengyel, and W. Riedmüller, in *Proceedings of the Fusion Fueling Workshop*, Princeton, New Jersey, 1977, CONF-771129 (unpublished).

<sup>3</sup>S. L. Milora and C. A. Foster, ORNL Report No. ORNL-TM-6598 (to be published).

<sup>4</sup>S. L. Milora and C. A. Foster, "A Revised Neutral Gas Shielding Model for Pellet-Plasma Interactions" (to be published).

<sup>5</sup>P. B. Parks, R. J. Turnbull, and C. A. Foster, *Nucl. Fusion* **17**, 539 (1977).

<sup>6</sup>D. F. Vaslow, *IEEE Trans. Plasma Sci.* **5**, 12 (1977).

<sup>7</sup>H. C. Howe, private communication.

## Evidence for a New Phase Transition in Solid $^3\text{He}$ in High Magnetic Fields

E. A. Schuberth,<sup>(a)</sup> D. M. Bakalyar, and E. D. Adams

*Physics Department, University of Florida, Gainesville, Florida 32611*

(Received 24 August 1978)

Liquid and solid  $^3\text{He}$  have been cooled by adiabatic compression to the solid ordering temperature in fields of 2.0 and 2.8 T. Chart traces of pressure versus time show a new feature which suggests a first-order transition near the  $A_1$ - $A_2$  superfluid transitions.

Exchange interactions in solid  $^3\text{He}$  are sufficiently strong to produce a magnetic transition of the nuclear spins to an ordered state at a much higher temperature than for classical dipoles. In several recent studies,<sup>1-3</sup> this phase transition has been observed near 1 mK. In low magnetic fields, the transition is antiferromagnetic and may possibly be first order.<sup>3,4</sup> In magnetic fields greater than 0.42 T, the melting pressure data of Kummer, Mueller, and Adams<sup>2</sup> (KMA) show that the ordering is of a different type. Thermodynamic analysis<sup>4</sup> of the KMA data suggests a second-order transition to a weakly ferromagnetic or pseudoferrromagnetic state. In the present work, the transition has been studied in magnetic fields of 2.0 and 2.8 T. The most striking result is the appearance of a new feature which suggests a phase transition in the solid near the  $A_1$  and  $A_2$  superfluid transitions.

A mixture of liquid and solid  $^3\text{He}$  was cooled

along the melting curve to a minimum of 0.85 mK (in low fields) using the Pomeranchuk compression cell described by KMA. The experiment consisted of qualitative observations of  $^3\text{He}$  pressure  $P_3$  versus time during the compressions, and of preliminary measurements of the latent heat of melting, from which the melting pressure and entropy versus temperature were obtained.

The new phase transition displays itself dramatically in the chart traces of  $P_3$  versus time shown in Fig. 1. The first curve is for  $B = 2.0$  T and all the others are for  $B = 2.8$  T but at different compression rates. Following the changes in slope at the  $A_1$  and  $A_2$  superfluid transitions<sup>5</sup> (indicated by arrows), a new feature appears as an abrupt backstep in pressure, which we believe indicates a new phase transition in solid  $^3\text{He}$ , as will be discussed below. (This backstep is similar to that seen at the superfluid  $B$  transition, suppressed for  $B > 0.5$  T.) On a given compression

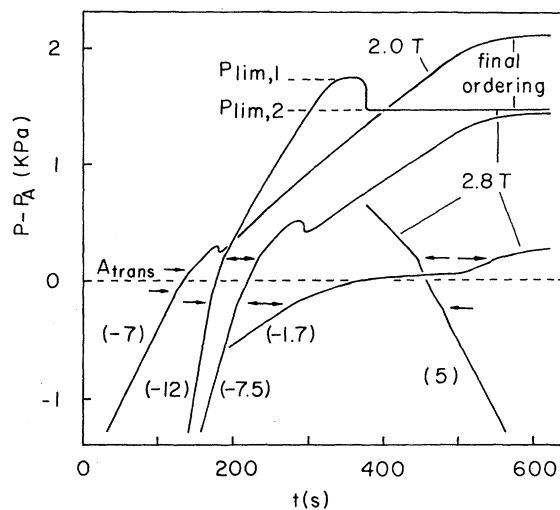


FIG. 1. Chart traces of  $^3\text{He}$  melting pressures during compressions. The arrows indicate the  $A_1$  and  $A_2$  superfluid transitions. Numbers in parentheses give the cooling or warming rate near  $T_A$  in microkelvins per second. The backsteps give evidence for a new phase transition in solid  $^3\text{He}$ . In the 2.8-T field, the two limiting pressures for the supercooled and equilibrium phases are shown by  $P_{\text{lim},1}$  and  $P_{\text{lim},2}$ .

only a single backstep in pressure was observed unless the cell was warmed to  $T \gtrsim T_A$ .

The pressure, hence temperature, of the feature depends on the compression rate, as indicated by the various curves shown for 2.8 T. At the slowest rate, it appeared as an almost flat portion of the chart trace, falling between  $A_1$  and  $A_2$  in both 2.0 and 2.8 T. This is apparently near the equilibrium position of the feature in these fields. At still slower rates the trace becomes too flat to identify the feature.

In the 2.8-T field, with a rapid compression rate ( $dT/dt = -12 \mu\text{K}/\text{sec}$  near  $T_A$ ), the backstep did not occur until the pressure had reached its limiting value  $P_{\text{lim},1}$ . This abrupt leveling of the pressure is characteristic of the ordering of the solid seen previously in fields  $\leq 1.2 \text{ T}$ .<sup>1,2</sup> Sometime after the leveling of the pressure at  $P_{\text{lim},1}$ , the backstep occurred, with the pressure dropping to a new, lower limiting value  $P_{\text{lim},2}$ . Once this had occurred, compression at an arbitrarily high rate would not raise the pressure above  $P_{\text{lim},2}$ . However, if the cell was warmed to  $T \gtrsim T_A$  and again compressed rapidly, the higher limiting pressure was observed, followed by the sequence described above.

A backstep in pressure could be caused by rapid warming of the cell if there are thermal

gradients which are smoothed out quickly following the superfluid transition. In this case it would then be possible to compress the cell back to the lower temperature and higher pressure seen before the warming. However, the behavior just described at the limiting pressure rules out this possibility and indicates that a new phase is being observed.

The new phase clearly leads to a different melting curve as indicated by the different limiting pressures of the solid ordering for  $B = 2.8 \text{ T}$  shown in Fig. 1. The lower limiting pressure and consequently lower  $|dP/dT|$  indicate a drop in the solid-liquid entropy difference when the transition occurs. This drop cannot originate from the liquid since it would mean an increase of the liquid entropy upon cooling. Thus the transition must take place in the solid. The dependence of the position of the step on the cooling rate may indicate supercooling, which implies that the transition would be of first order. When the transition takes place from the supercooled state, the latent heat would produce warming, which, combined with a lower melting pressure, gives the backstep in pressure. The almost-flat portion in the slowest compression shown in Fig. 1 ( $dT/dt = -1.7 \mu\text{K}/\text{sec}$ ) presumably indicates the latent heat of a first-order transition taking place without supercooling. On warming, a flat portion would then also be expected, but was not observed. The only indication of the transition was more pronounced upward curvature in the chart traces in the vicinity of the  $A$  transitions.

The above behavior could be explained by thermal gradients and the absence of superheating. On warming, the transition would be smeared out as each portion of the solid is warmed through the transition temperature. On cooling at high compression rates, the transition would take place abruptly through the supercooled solid once it is initiated. In a slow compression in which the transition takes place without supercooling, thermal gradients would cause the transition in the interior to occur after that at the surface while the melting pressure would continue to increase in the compression. This is the behavior seen in the slowest trace in Fig. 1. When the effect of heat leaks is considered, the horizontal displacements of the extrapolated chart traces before and after the transition are about the same on warming as on cooling.

The height of the backstep was measured by taking the difference in the extrapolated pressure just before and after the step. This height

increased with the degree of supercooling, was greater for 2.8 T than for 2.0 T, but showed no systematic dependence on time during a compression and thus on the amount of solid present. An indication of the heat removed in the transition was obtained by measuring the quantity of heat which had to be supplied to produce the same horizontal displacement in the chart trace. This was  $\sim 20$  and  $40$  ergs at  $2.5$  mK for the  $2.0$ - and  $2.8$ -T fields, respectively. The cell contained about  $0.25$  moles of  $^3\text{He}$ , of which about  $25$ – $50\%$  was solid during the observations of the transition.

Preliminary measurements have been made of the latent heat of melting per unit volume,  $\Delta Q/\Delta V$ , from which the melting temperature and entropy are obtained. The melting temperature is given by<sup>1</sup>

$$T = T_0 \exp \int_{P_0}^P (\Delta V/\Delta Q) dP, \quad (1)$$

where  $(T_0, P_0)$  is some fixed point. For the fixed point we took the field-independent value of  $T_A(B=0) = T_A(B) = 2.68$  mK,<sup>2</sup> defined by<sup>6</sup>

$$T_A(B) = 0.375T_{A_1} + 0.625T_{A_2}. \quad (2)$$

For the temperature splitting with field,  $(T_{A_1} - T_{A_2})/B$ , we found  $61.0 \pm 5.0$   $\mu\text{K}/\text{T}$  up to  $2.0$  T, in agreement with the  $64$   $\mu\text{K}/\text{T}$  found previously.<sup>5,6</sup> This splitting was no longer linear at the higher field of  $2.8$  T where it had increased to  $74.5 \pm 5.0$   $\mu\text{K}/\text{T}$ . The error quoted here is almost entirely in the temperature scale. Support for this re-

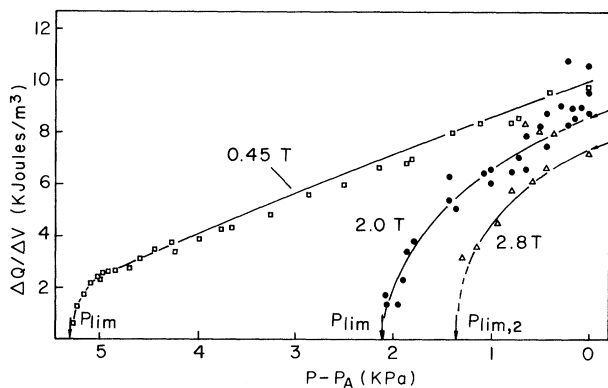


FIG. 2. Latent heat of melting (raw data) vs pressure differences below the A transition at  $T_A = 2.68$  mK. The arrows along the abscissa show the limiting (equilibrium) pressures reached in each compression. The arrows to the right of the  $2.0$ - and  $2.8$ -T data show the values of  $\Delta Q/\Delta V$  required to produce the observed change in  $P_A$  with field in integrating  $dP/dT$  from high  $T$  to  $T_A$  with  $S$  proportional to  $T^{-2}$ .

sult is given by the pressure splitting,  $(P_{A_2} - P_{A_1})/B$ , which increased faster than linear, implying a still faster temperature splitting since the melting curve slope is lower at the higher fields. The nonlinear behavior is of interest itself and requires further study. The decrease in melting pressure at  $T_A$  with field was given by  $524B^2$  ( $\text{Pa}/\text{T}^2$ ) to the highest field of  $2.8$  T, following the trend seen by Osheroff<sup>7</sup> at lower fields.

Long time constants and hysteresis were encountered in the measurements of  $\Delta Q/\Delta V$  in the vicinity of the new transition (i.e., near  $T_A$  of the liquid) and to a lesser degree at higher temperatures. Consequently, the data were reliable only in the region below  $T_A$ . These are shown in Fig. 2, where the smooth curves through the data were used to perform the numerical integration in Eq. (1). The resulting melting curves  $P(T)$  are presented in Fig. 3. Errors in  $T$  are determined by the accuracy of the area under the  $\Delta Q/\Delta V$  curves below the reference temperature  $T_0$  [see Eq. (1)]. Since  $T_0$  was taken as  $T_A$ , the accumulated errors in  $T$  (relative to  $T_A$ ) are only

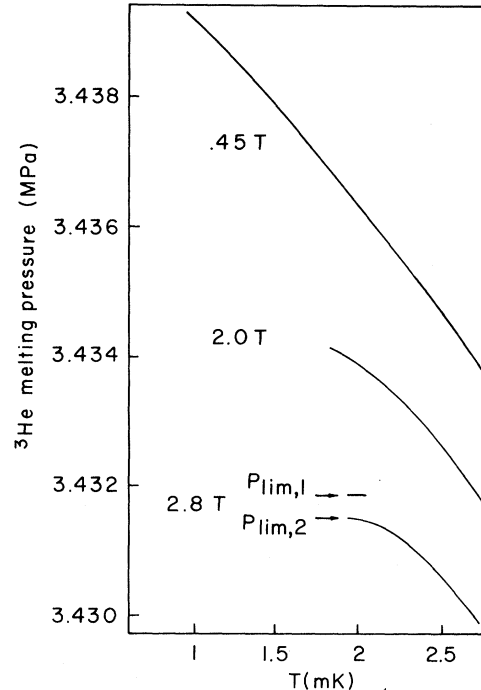


FIG. 3. Melting pressures vs temperature of  $^3\text{He}$  below the A transition. For  $2.8$  T, the limiting pressures reached at the solid ordering in the supercooled and equilibrium phases are indicated by  $P_{\text{lim},1}$  and  $P_{\text{lim},2}$ , respectively.

about  $\pm 0.05$  mK at the solid ordering. Using  $dP/dT$  from the curves of Fig. 3, the  $\Delta Q/\Delta V$  data, and the liquid entropy, the solid entropy was obtained (not shown). From these curves, ordering temperatures of 1.9 and 2.15 mK are indicated for the 2.0- and 2.8-T fields, respectively. points follow the trend established by KMA (Ref. 2) for fields between 0.4 and 1.2 T. Unfortunately, the hysteresis and long time constants near the transition temperature do not permit reliable conclusions on the behavior of the entropy in this region. Furthermore, the above estimate of the latent heat in the transition indicates only a very small change in entropy.

Following the analysis of Adams, Delrieu, and Landesman,<sup>4</sup> the magnetic susceptibility can be found from the relation

$$\chi_{B_1, B_2} = \left( \frac{2\Delta v}{v} \right) \frac{P_m(B_1) - P_m(B_2)}{B_2^2 - B_1^2}. \quad (3)$$

Here  $v$  is the molar volume of the solid at melting and  $\Delta v$  is the difference in molar volume between the liquid and solid. Using  $B_1 = 2.0$  T and  $B_2 = 2.8$  T, we find  $\chi = 6.3 \times 10^{-6}$  and  $5.5 \times 10^{-6}$  at  $T = 2.1$  and 2.6 mK, respectively. These values are in good agreement with those obtained in Ref. 4 from the data of Ref. 2 for lower fields.

In this work, the chart traces of pressure versus time have given evidence of a second phase transition in the solid in high fields. However,

further work is required for an understanding of the magnetic phases of solid  $^3\text{He}$ . To aid in determining the type of spin ordering involved, we are preparing NMR experiments in conjunction with further latent-heat measurements.

We acknowledge useful discussion with E. B. Flint and G. G. Ihas. One of us (D.M.B.) thanks W. P. Halperin for fruitful conversations concerning these results. This work was supported by the National Science Foundation and partly by the Deutsche Forschungsgemeinschaft.

<sup>(a)</sup>On leave from Fachbereich Physik, Universität Regensburg, Regensburg, West Germany.

<sup>1</sup>W. P. Halperin, C. N. Archie, F. B. Rasmussen, R. A. Buhrmann, and R. C. Richardson, *Phys. Rev. Lett.* **32**, 927 (1974), and **34**, 718 (1975).

<sup>2</sup>R. B. Kummer, R. M. Mueller, and E. D. Adams, *J. Low Temp. Phys.* **27**, 319 (1977).

<sup>3</sup>T. C. Prewitt and J. M. Goodkind, *Phys. Rev. Lett.* **39**, 1283 (1977).

<sup>4</sup>E. D. Adams, J. M. Delrieu, and A. Landesman, *J. Phys. (Paris), Lett.* **39**, L190 (1978).

<sup>5</sup>W. J. Gully, D. D. Osheroff, D. T. Lawson, R. C. Richardson, and D. M. Lee, *Phys. Rev. A* **8**, 1633 (1973).

<sup>6</sup>D. D. Osheroff and P. W. Anderson, *Phys. Rev. Lett.* **33**, 686 (1974).

<sup>7</sup>D. D. Osheroff, thesis, Cornell University Report No. 1932, 1972 (unpublished).

## Al Surface Relaxation Using Surface Extended X-Ray-Absorption Fine Structure

A. Bianconi

*Istituto di Fisica, Università di Camerino, Camerino, Italy, and Stanford Synchrotron Radiation Laboratory, Stanford University, Stanford, California 94305*

and

R. Z. Bachrach

*Xerox Palo Alto Research Center, Palo Alto, California 94304*

(Received 2 March 1978)

The surface extended x-ray-absorption fine structure (EXAFS) of a single crystal has been measured for the first time. By comparison with parameters obtained from bulk aluminum EXAFS, a decrease of the interatomic distance ( $\Delta r = 0.15 \pm 0.05$  Å) at the Al(111) surface has been found. No relaxation is found of the Al-Al separation on the (100) face.

The difficulty of determining surface structure is one of the greatest barriers to the development of a better understanding of surface electronic states and bonding.<sup>1</sup> Low-energy electron diffraction (LEED)<sup>2</sup> is essentially the one estab-

lished technique for structure determination. This technique is limited to single-crystal analysis or chemisorbed atoms with a long-range order and has a low resolution. Recently by using synchrotron radiation as a source for x-ray spec-